

STICHTING  
MATHEMATISCH CENTRUM  
2e BOERHAAVESTRAAT 49  
AMSTERDAM

TW 84

The North Sea Problem VIII

A numerical treatment

H.A. Lauwerier  
B.R. Damste



1962

## The North Sea Problem VIII

### A numerical treatment <sup>1)</sup>

by

H.A. Lauwerier and B.R. Damsté

#### 1. Introduction <sup>2)</sup>

In this paper we consider some results obtained by purely numerical methods concerning the rectangular model of the North Sea which has been considered in the previous publications in this series. These results could be obtained by using the X1-computer of the Mathematical Centre in working out the many iterations needed in a three-dimensional difference scheme. It has been said in the introduction of the previous paper that the analytical treatment did not consider the important effects of a non-constant depth and inhomogeneities of the windfield. Of course something could be done in connection with these effects by analytical means, but here it seems we have reached the limit of where the analytical method can give us useful information in an economical way. On the other hand the numerical method does not replace the analytical method, but rather supplements it. Moreover in each individual special case the numerical method may take into account all sorts of variations and refinements of the standard model. Therefore a numerical scheme has been constructed by means of which it is possible to calculate both stream and elevation in the rectangular model of the North Sea with an adaptable depth profile  $h(x,y)$  and for a sufficiently wide class of inhomogeneous windfields. Of course we did not fully exploit this freedom of choice in the numerical model. So far we considered only a model with a constant depth and one with a depth function varying exponentially as described in N.S.P. III.

Further we considered only windfields of a very special type, as will be described below. By selecting a number of typical cases we are able,

-----  
1) Report TW 84 of the Mathematical Centre, Amsterdam.

2) The notation is the same as in the previous publications of this series.



with due reservation, to discuss the influence of a variation of the bottom profile and the inhomogeneity of the windfield.

Historically, our first objective was to set up a stable difference scheme which approximates the differential equations of the model. According to (I 2.6) and (I 2.7) they are

$$(1.1) \quad \begin{cases} \frac{\partial u}{\partial t} = -\lambda u + \Omega v - gh \frac{\partial \zeta}{\partial x} + U(x,y,t) \\ \frac{\partial v}{\partial t} = -\lambda v - \Omega u - gh \frac{\partial \zeta}{\partial y} + V(x,y,t) \\ \frac{\partial \zeta}{\partial t} = -\frac{\partial u}{\partial x} - \frac{\partial v}{\partial y} , \end{cases}$$

with the boundary conditions

$$(1.2) \quad \begin{cases} u = 0 & \text{for } x = 0 \text{ and } x = a, \\ v = 0 & \text{for } y = 0 , \\ \zeta = 0 & \text{for } y = b , \end{cases}$$

and with a given situation at  $t=0$ .

In this model the parameters  $\lambda$  and  $\Omega$  are assumed to be constants. The depth  $h$  may be a function of  $x$  and  $y$ .

The difference scheme may be written symbolically as

$$(1.3) \quad u, v, \zeta(t+\tau) = F\{u, v, \zeta(t)\} ,$$

where  $\tau$  is the elementary time-step.

The authors met a number of difficulties here for they observed that some difference schemes which were stable for  $\Omega = 0$  developed instabilities when they were used with  $\Omega \neq 0$ . Stability analysis along the lines of von Neumann, Lax and Richtmyer is only possible for  $\Omega = 0$ , or for  $\Omega \neq 0$  only without boundary conditions. Yet a stable system has been constructed and will be described in detail in section 2. Some stability analysis will be given in section 3. A characteristic of our difference scheme seems to be the introduction of an "artificial viscosity" induced by locally averaging or smoothing.

In section 4 the numerical scheme is shown to give the same or almost the same results as the analytical treatment of N.S.P. VI and VII. In order to facilitate comparison we use throughout this paper the same units and standard values. I.e.

$$(1.4) \quad \left\{ \begin{array}{l} a = \pi, \quad b = 2\pi, \quad \text{harm.av. (gh)} = 1, \\ \Omega = 0.6, \quad \lambda = 0.12, \\ \max (U^2 + V^2)^{\frac{1}{2}} = 1. \end{array} \right.$$

With these values the dimensionless time scale is 1.4 hours pro unit. According to VII section 4 we consider the step-sine windfield

$$(1.5) \quad U = 0 \quad V = -\sin \omega t \quad \text{for } t > 0$$

with  $\omega = 0.1$ .

For the case  $\Omega = 0$ , for which an exact analytical expression is available, the numerical method gives the same results as the analytical method.

For  $\Omega \neq 0$  the values of  $\zeta(\frac{1}{2}\pi, 0, t)$  have been calculated in VII table 8. They are compared here with results obtained by the numerical method. Table 1 and figure 2 show that the agreement is indeed surprisingly good. This provides us with a non-trivial check of the adequacy of either method.

In order to judge the influence of the depth profile the same calculations have been repeated for the windfield (1.5) and the exponential depth profile

$$(1.6) \quad h = h_0 e^{\alpha y}, \quad \alpha = \frac{1}{4}.$$

Values of  $\zeta(\frac{1}{2}\pi, 0, t)$  are given in table 1 and figure 2. The influence of the change in the depth profile is apparent. The maximum elevation at  $(\frac{1}{2}\pi, 0)$  is slightly higher and is reached somewhat sooner. The various values of this maximum are as follows

approximate analytic expression	5.93
numerical method, uniform depth	6.13
numerical method, exponential depth	6.66
stationary value	$2\pi$



From the values of  $\zeta(x,y,t)$  which are calculated at  $12 \times 24$  points of the sea at various times we have constructed a number of "snapshots" showing lines of equal elevation. These are given in figure 3 for the case of a uniform depth and in figure 4 for an exponential depth.

Similar calculations have been performed for a "west wind" of the type

$$(1.7) \quad U = \sin \omega t, \quad V = 0 \quad \text{for } t > 0$$

again with  $\omega = 0.1$ . This enables us to estimate the influence of the direction of the wind when the intensity is kept constant. Values of  $\zeta(\frac{1}{2}\pi, 0, t)$  are given in table 2 for the case of an exponential depth profile. The most unfavourable direction for a storm as regards the elevation at  $(\frac{1}{2}\pi, 0)$  is one which makes an angle of  $12\frac{1}{2}^\circ$  with the positive Y-axis. For the North Sea this would mean a deviation of some  $25^\circ$  from the North in Western direction. The maximum elevation at  $(\frac{1}{2}\pi, 0)$  is now 6.83 which is to be compared with the value 6.66 for a purely "Northern" wind. Thus the directional effect is about 3% which is rather small.

The same calculations have been carried out for a number of non-homogeneous windfields of the type

$$(1.8) \quad U, V = L(x,y) \sin \omega t, \quad t > 0,$$

where  $L$  is a linear function of  $x$  and  $y$  and where again  $\omega = 0.1$ . In view of the superposition principle - we deliberately took a linear model - a great variety of non-homogeneous windfields may be considered by calculating only a few typical cases. In order to enable the reader to calculate the elevation at  $(\frac{1}{2}\pi, 0)$  for some particular linear windfield of the type (cf. II 5.1)

$$(1.9) \quad \begin{cases} U = (a_1 + b_1 x + c_1 y) \sin \omega t \\ V = (a_2 + b_2 x + c_2 y) \sin \omega t \end{cases}$$

some data are given in table 3.

In section 5 the influence of changes in  $\lambda$  and  $\omega$  are considered. A number of calculations have been performed for the rectangular

model with the exponential depth function (1.6) and for the homogeneous Northern windfield (1.5). Table 4 and figure 5 show the elevation at  $(\frac{1}{2}\pi, 0)$  at the critical period when the elevation is highest. It appears that the maximum elevation at  $(\frac{1}{2}\pi, 0)$  is rather insensitive to relatively large changes in  $\lambda$  such as  $0.10 \leq \lambda \leq 0.14$ . This is a very fortunate fact since in reality the coefficient of friction is some function of the depth about which little is known.

Similar calculations have been carried out with the standard value  $\lambda = 0.12$  but with  $\omega$ -values 0.08 (0.02) 0.20. This means that we consider a range of storms with a duration between 22 hours and 55 hours but with the same peak intensity. Values of  $\zeta(\frac{1}{2}\pi, 0, t)$  are collected in table 5 and a graphical illustration is given in figure 6. There appears to be a slight resonance effect at  $\omega = 0.15$ . In figure 7 the maximum elevation at  $(\frac{1}{2}\pi, 0)$  is plotted as a function of  $\omega$ . The maximum of this function is not very pronounced, which seems to be due to the relatively large value of the friction term. However, for  $\omega = 0.15$  a maximum elevation at  $(\frac{1}{2}\pi, 0)$  is obtained of 6.83 which may be compared to the value 6.66 obtained earlier. If to this the directional effect is added a round figure of 7.00 is obtained for a uniform windfield with the most unfavourable direction and period.

In section 6 as a separate topic the after-effect of a sudden disturbance is considered. As a model it is assumed that a uniform and constant Northern wind, for which the sea has come into its equilibrium situation, suddenly stops. As a result of this a damped oscillatory motion develops which practically disappears after some 21 hours. Values of  $\zeta(\frac{1}{2}\pi, 0, t)$  are given in table 6 and the corresponding graph is presented in figure 8.

Finally in section 7 the ALGOL version of the numerical process is given in detail.



## 2. The difference scheme

The differential equations (1.1) will be replaced by the following difference scheme

$$(2.1) \left\{ \begin{array}{l} u(x, y, t+\tau) = (1-\lambda\tau)u(x, y, t) + \Omega\tau v(x, y, t) - gh\tau\xi^{-1}D_1\zeta(x, y, t) + \\ \quad + \tau U(x, y, t) \\ v(x, y, t+\tau) = (1-\lambda\tau)v(x, y, t) - \Omega\tau u(x, y, t) - gh\tau\eta^{-1}D_2\zeta(x, y, t) + \\ \quad + \tau V(x, y, t) \\ \zeta(x, y, t+\tau) = -\tau\xi^{-1}D_1u(x, y, t) - \tau\eta^{-1}D_2v(x, y, t) + \zeta(x, y, t), \end{array} \right.$$

where the difference operators  $D_1$  and  $D_2$  are averages of central difference operators in the following sense:

$$(2.2) \left\{ \begin{array}{l} D_1 f(x, y) = \xi^{-1} \cdot \frac{1}{2} \left\{ \left( \frac{\Delta f}{\Delta x} \right)_{(x, y+\eta)} + \left( \frac{\Delta f}{\Delta x} \right)_{(x, y-\eta)} \right\} = \\ \quad = \frac{1}{4} \{ f(x+\xi, y+\eta) - f(x-\xi, y+\eta) + f(x+\xi, y-\eta) - f(x-\xi, y-\eta) \} \\ D_2 f(x, y) = \eta^{-1} \cdot \frac{1}{2} \left\{ \left( \frac{\Delta f}{\Delta y} \right)_{(x+\xi, y)} + \left( \frac{\Delta f}{\Delta y} \right)_{(x-\xi, y)} \right\} = \\ \quad = \frac{1}{4} \{ f(x+\xi, y+\eta) - f(x+\xi, y-\eta) - f(x-\xi, y+\eta) + f(x-\xi, y-\eta) \}. \end{array} \right.$$

The elementary mesh  $(\xi, \eta)$  of  $R$  is determined by dividing  $a$  in  $2m$  equal parts and  $b$  in  $2n+1$  equal parts,

$$(2.3) \quad \xi = \frac{a}{2m}, \quad \eta = \frac{b}{2n+1}.$$

The stream and the elevation are calculated at different points which form two interlacing nets as shown in figure 1, where the crosses denote points where the components of the stream are calculated and the dots points where the elevation is calculated.

At the boundary of  $R$  some supplementary definition with respect to  $\zeta$  of the difference operators  $D_1$  and  $D_2$  is needed.

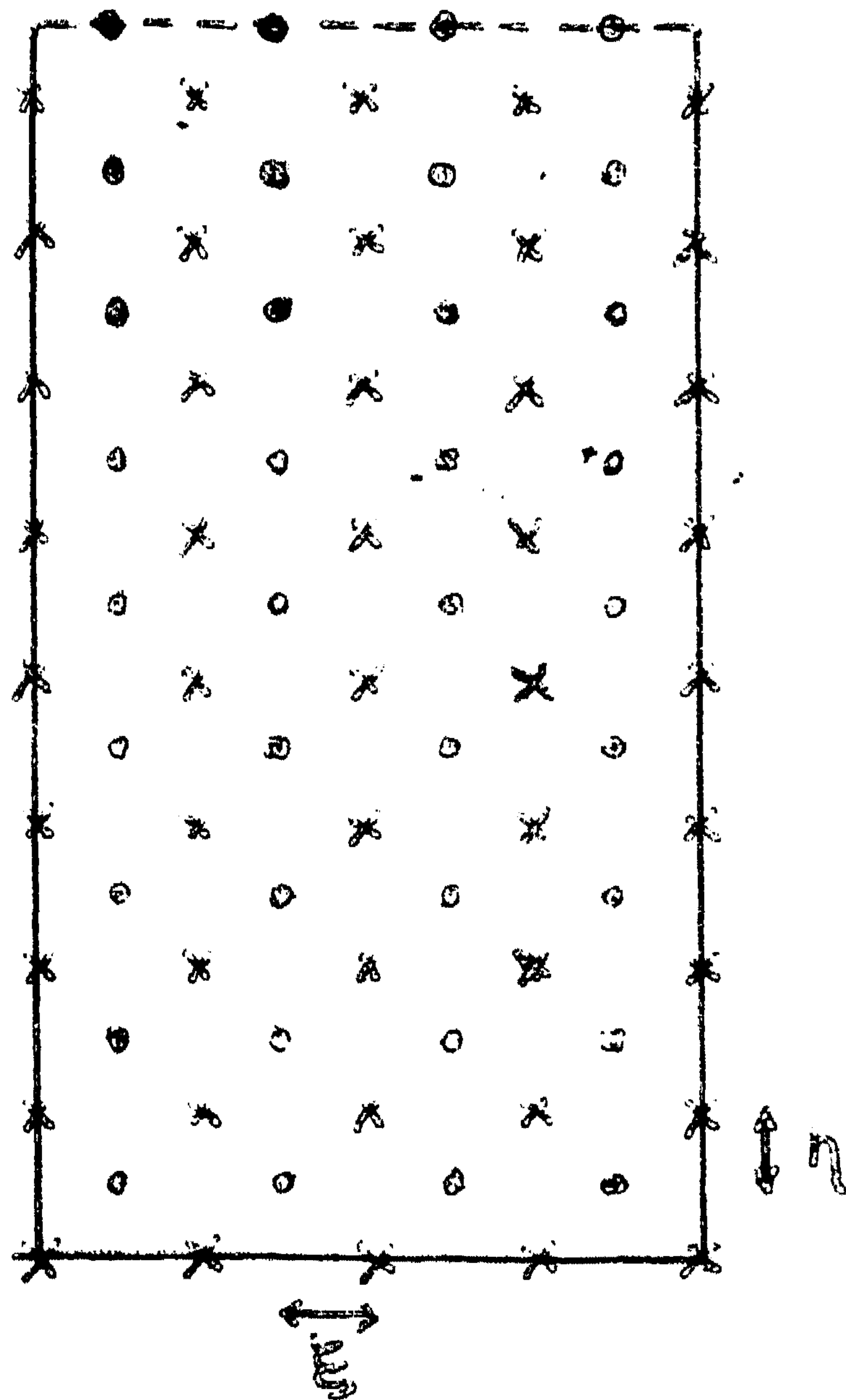


fig.1 This figure applies to the case  
m=4, n=8

- o Points at which  $f$  is computed
- x Points at which  $u, v$  are computed

We may take the following simple definitions

$$(2.4) \quad \begin{cases} D_1 f(x, 0) = \frac{1}{4} \{ f(x+\xi, \eta) - f(x-\xi, \eta) \} \\ D_2 f(0, y) = \frac{1}{4} \{ f(\xi, y+\eta) - f(\xi, y-\eta) \} \\ D_2 f(a, y) = \frac{1}{4} \{ f(a-\xi, y+\eta) - f(a-\xi, y-\eta) \} . \end{cases}$$

However, in the actual computations we used a slightly modified version, as is shown in the ALGOL procedure (section 7).

The difference scheme (2.1) may be considered as an operator which transforms the situation at some time  $t$  into the situation at the later instant  $t+\tau$ . The numerical solution of the difference scheme is merely the iterative application of this operator when starting from the given situation at  $t=0$ . If this is a stable procedure we know that a solution of the difference scheme is obtained which approximates a solution of the original differential equations, the degree of approximation depending on the width of the mesh  $(\xi, \eta)$  and the magnitude of the time step  $\tau$ . A complete theoretical discussion of the stability will not be given here. In the following section a sufficient condition will be derived only for the important subcase of a uniform depth. Neglecting boundary conditions, this condition guarantees what may be called internal stability. We found, however, using a given mesh size, i.e. with fixed values of  $m$  and  $n$ , that the system always become stable if  $\tau$  was taken sufficiently small. In most cases we took the values  $m=12$  and  $n=24$  which correspond to an



almost square mesh  $(\xi, \eta)$  with a side of 9 miles, and a time step  $\tau = 1/16$ , which comes to abt. 5 min.

### 3. Stability analysis

We shall apply the well-known method of von Neumann which consists in introducing at some time  $t$  an arbitrary small disturbance, periodic in space, and discussing the possible growth of the disturbance at the next instant  $t+\tau$  by considering the eigenvalues of the so-called amplification matrix. When applying this method, the external forces may be neglected. However, we must make the following two restrictions. In the first place we neglect the boundary conditions, i.e. the region is extended to infinity, and secondly the depth is assumed to be constant.

As the initial situation we take the following small disturbance

$$(3.1) \quad \begin{cases} u = m_1 \sqrt{gh} \exp i(\sigma_1 x + \sigma_2 y) \\ v = m_2 \sqrt{gh} \exp i(\sigma_1 x + \sigma_2 y) \\ \zeta = m_3 \exp i(\sigma_1 x + \sigma_2 y) \end{cases} .$$

Substitution of this into (2.1) gives at the next instant  $t = \tau$

$$(3.2) \quad \begin{cases} u/\sqrt{gh} = \alpha m_1 + \beta m_2 - i \gamma_1 m_3 \\ v/\sqrt{gh} = -\beta m_1 + \alpha m_2 - i \gamma_2 m_3 \\ \zeta = -i \gamma_1 m_1 - i \gamma_2 m_2 + m_3 \end{cases} ,$$

where

$$(3.3) \quad \alpha = 1 - \lambda \tau, \quad \beta = \Omega \tau, \quad \gamma_1 = \tau \xi^{-1} \sin \sigma_1 \xi \cos \sigma_2 \eta, \\ \gamma_2 = \tau \eta^{-1} \cos \sigma_1 \xi \sin \sigma_2 \eta.$$

The eigenvalue equation of the amplification matrix is

$$(1-s) \{ (\alpha-s)^2 + \beta^2 \} + (\alpha-s)(\gamma_1^2 + \gamma_2^2) = 0$$

or

$$(3.4) \quad s^3 + a_1 s^2 + a_2 s + a_3 = 0,$$

where

$$(3.5) \quad a_1 = -1-2\alpha, \quad a_2 = \alpha^2 + 2\alpha + \beta^2 + \gamma_1^2 + \gamma_2^2, \\ a_3 = -\alpha^2 - \beta^2 - \alpha\gamma_1^2 - \alpha\gamma_2^2.$$

The stability condition is that all three roots of (3.4) are within the unit circle for all possible values of  $\gamma_1$  and  $\gamma_2$ , i.e. in the range

$$(3.6) \quad 0 \leq \gamma_1^2 + \gamma_2^2 \leq \tau^2(\xi^{-2} + \eta^{-2}).$$

The latter condition can be expressed in the form of a number of inequalities which easily follow from the well-known Hurwitz criterion. We must have

$$(3.7) \quad \begin{cases} 1 + a_1 + a_2 + a_3 > 0 \\ 1 - a_1 + a_2 - a_3 > 0 \\ 3 + a_1 - a_2 - 3a_3 > 0 \\ 1 - a_2 + a_1 a_3 - a_3^2 > 0. \end{cases}$$

A simple calculation shows that for  $\alpha > 1/3$  the first three inequalities are satisfied. The last inequality gives

$$(3.8) \quad \alpha^2(\gamma_1^2 + \gamma_2^2)^2 - \{ (1-\alpha)(2\alpha^2-1) - 2\alpha\beta^2 \} (\gamma_1^2 + \gamma_2^2) + \\ - (1-\alpha^2 - \beta^2) \{ (1-\alpha)^2 + \beta^2 \} < 0.$$

Since this also holds for  $\gamma_1 = \gamma_2 = 0$  it follows that

$$(3.9) \quad \alpha^2 + \beta^2 < 1.$$

The inequality (3.8) may be replaced by

$$(3.10) \quad 2\alpha^2(\gamma_1^2 + \gamma_2^2) < (1-\alpha)(2\alpha^2-1) + (1-\alpha)^{\frac{1}{2}}(1-\alpha+4\alpha\beta^2)^{\frac{1}{2}}.$$

A sufficient condition is clearly obtained if we take  $\beta = 0$ . Then we



obtain

$$(3.11) \quad \eta_1^2 + \eta_2^2 \leq 1 - \alpha.$$

Hence there is stability for

$$(3.12) \quad \left( \frac{1}{\xi^2} + \frac{1}{\eta^2} \right) \tau \leq \lambda \quad \text{with} \quad \tau \leq \min \left( \frac{2}{3\lambda}, \frac{2\lambda}{\lambda^2 + \Omega^2} \right).$$

We notice the fact that for  $\lambda=0$  the process is always unstable.

The stability criterion (3.12) does not guarantee stability when the true boundary conditions are taken into account. A number of trials of the difference scheme on the electronic computer showed that with an appropriately small mesh the boundary conditions were still compatible with stability. Clearly, some research remains to be done on this subject.

#### 4. Comparison of analytical and numerical results

a. We first considered the analytical model of N.S.P. VI and VII. In particular we considered the elevation  $\zeta(\frac{1}{2}\pi, 0, t)$  at the middle of the "Dutch" coast of the rectangular sea  $0 < x < \pi$ ,  $0 < y < 2\pi$ , due to a homogeneous step-sine wind (cf. VII 4.1)

$$(4.1) \quad U = 0 \quad V = -\sin \omega t \quad \text{for} \quad t > 0$$

with  $\omega = 0.1$ .

Since for  $\Omega = 0$  an exact expression is available (VII 4.6 and 4.8) we first checked the numerical scheme by calculating the elevation at  $y=0$  for this value of the Coriolis parameter. The results were found to be in excellent agreement. Next we calculated  $\zeta(\frac{1}{2}\pi, 0, t)$  with due regard of the Coriolis parameter  $\Omega = 0.6$ . The results are given in table 1 and figure 2 (p.20).

We note a striking agreement between the results obtained by the analytical method of N.S.P. VI and VII and the numerical method. (It is interesting to note here that when we first compared the two results an error was discovered in the analytical result.)

t	anal.	numer.	exp.depth
0	0	0	0
3	-	0.40	0.52
6	1.50	1.49	1.81
9	3.08	3.07	3.73
12	4.41	4.52	5.36
15	5.38	5.58	6.38
18	5.88	6.09	6.66
21	5.86	6.08	6.23
24	5.33	5.46	5.33
27	4.34	4.45	4.04
30	2.96	2.94	2.27

Table 1. Elevations at  $(\frac{1}{2}\pi, 0)$ . Windfield  $\begin{cases} U = 0 \\ V = -\sin 0.1t \end{cases}$   
 $\omega = 0.12$ ,  $\Omega = 0.6$

anal.: elevation for uniform depth, obtained by analytical means  
numer.: " " " " " " purely numerical means  
exp. depth: " " exponential depth, obtained by " "

The numerical computation yielded each time the elevation at all 12 x 24 grid points. These figures were used to construct a number of pictures showing isohypses at some instants. The results are given in figure 3 (p.21) and may be compared to the similar pictures of VII fig.2 obtained by analytical means. Again the influence of the rotation of the Earth is obvious.

b. The same calculations were performed for the rectangular sea with the exponential depth profile (1.6). Table 1 and figure 2 (p.20) give in particular the elevation at  $(\frac{1}{2}\pi, 0)$ . Figure 4 (p.21) gives the isohypses as in the former case. We see that the overall picture is hardly affected by changing the depth profile. However, in the Southern part the maximum elevation, say at  $(\frac{1}{2}\pi, 0)$ , is significantly higher than in the previous case.

c. In order to determine the influence of the direction of the wind upon the elevation at the "Dutch" coast we considered the uniform step-sine windfield



$$(4.2) \quad U = \sin 0.1t, \quad V = 0 \quad \text{for } t \geq 0$$

upon the rectangular model with the exponential depth profile (1.6). The values of  $\zeta(\frac{1}{2}\pi, 0, t)$  are given in table 2.

t	$\zeta(\frac{1}{2}\pi, 0, t)$	t	$\zeta(\frac{1}{2}\pi, 0, t)$
0	0	18	1.45
3	0.26	21	1.47
6	0.50	24	1.19
9	0.80	27	0.95
12	1.18	30	0.66
15	1.41		

Table 2: Elevations at  $(\frac{1}{2}\pi, 0)$ , windfield  $\begin{cases} U = \sin 0.1t \\ V = 0 \end{cases}$

Exponential bottom profile,  $\lambda=0.12$ ,  $\Omega = 0.6$

The previous results may be combined in order to find the elevation due to the windfield

$$(4.3) \quad U = \sin \alpha \sin 0.1t, \quad V = -\cos \alpha \sin 0.1t, \quad t \geq 0$$

for any value of the direction  $\alpha$  according to the formula

$$(4.4) \quad \zeta(\alpha) = \cos \alpha \zeta(0) + \sin \alpha \zeta(90^\circ).$$

The most unfavourable direction as regards the elevation at  $(\frac{1}{2}\pi, 0)$  is easily found to be  $\alpha=12\frac{1}{2}^\circ$  with the absolute maximum of  $\zeta(12\frac{1}{2}^\circ) = 6.83$  occurring at abt.  $t=18$ .

d. Similar calculations have been performed for non-homogeneous windfields of the type

$$(4.5) \quad U = 0 \quad V = -(1 - \frac{2x}{\pi}) \sin 0.1t$$

and

$$(4.6) \quad U = 0 \quad V = -(1 - \frac{y}{2\pi}) \sin 0.1t$$

and also

$$(4.7) \quad U = (1 - \frac{2x}{\pi}) \sin 0.1t \quad V = 0$$

and

$$(4.8) \quad U = (1 - \frac{y}{2\pi}) \sin 0.1t \quad V = 0.$$

The corresponding values of  $\zeta(\frac{1}{2}\pi, 0, t)$  for a number of  $t$  values are given in table 3. They are indicated by  $\zeta_1, \zeta_2, \zeta_3, \zeta_4$  in the above-given order. By linear combination the value of  $\zeta(\frac{1}{2}\pi, 0, t)$  may now be obtained for a great variety of non-homogeneous windfields.

t	$\zeta_1$	$\zeta_2$	$\zeta_3$	$\zeta_4$
0	0	0	0	0
3	0.01	0.46	0.16	0.24
6	0.36	1.41	0.30	0.44
9	0.91	2.51	0.41	0.69
12	1.45	3.41	0.57	0.89
15	1.92	4.00	0.70	1.03
16	2.04	4.04	0.71	1.00
17	2.16	4.06	0.73	0.99
18	2.23	4.06	0.74	1.00
19	2.27	4.02	0.73	1.02
20	2.31	3.91	0.71	1.02
22	2.32	3.63	0.69	0.97
24	2.25	3.20	0.61	0.88
26	2.08	2.62	0.52	0.77
28	1.85	1.96	0.41	0.60
30	1.53	1.25	0.28	0.48

Table 3: Elevations at  $(\frac{1}{2}\pi, 0)$ . Windfields (4.5), (4.6), (4.7) and (4.8) respectively

Exponential bottom profile,  $\lambda = 0.12$ ,  $\Omega = 0.6$ .



### 5. Influence of $\lambda$ and $\omega$

In order to get some information as regards the influence of variations of  $\lambda$  and  $\omega$  upon the elevation, and in particular the elevation at the "Dutch" coast, we took the standard case of a step-sine windfield (4.1) upon the rectangular model with the exponential depth profile (1.6). From the numerous data obtained by the electronic computer the following tables may be composed. Table 4 gives  $\zeta(\frac{1}{2}\pi, 0, t)$  at some typical times for the  $\lambda$  values 0.10, 0.12 and 0.14. These data are plotted in figure 5 (p. 22). It appears that the maximum elevation is rather insensitive to such changes in  $\lambda$ .

t	$\lambda = 0.10$	$\lambda = 0.12$	$\lambda = 0.14$
12	5.41	5.31	5.21
15	6.43	6.33	6.24
18	6.67	6.62	6.57
21	6.22	6.23	6.23

Table 4: Elevations at  $(\frac{1}{2}\pi, 0)$  for various values of  $\lambda$ .

$$\text{Windfield } \begin{cases} U=0 \\ V=-\sin 0.1t \end{cases}$$

Exponential bottom profile,  $\Omega = 0.6$ .

Table 5 gives  $\zeta(\frac{1}{2}\pi, 0, t)$  at various times for the  $\omega$  values 0.08, 0.10, 0.12, 0.14, 0.16, 0.18, 0.20.

The corresponding graphs are plotted in figure 6 (p. 23). It appears that the maximum elevation is a function of  $\omega$  which has its maximum near  $\omega = 0.15$ . This function has been plotted in figure 7 (p. 24). We note that for  $\omega \rightarrow 0$  this function tends to  $2\pi$  since for  $\omega \rightarrow 0$  the motion becomes quasi-stationary.

The maximum of the latter function is not very pronounced. It may be expected that for smaller values of  $\lambda$ , i.e. smaller friction parameter, this resonance effect will be stronger.

$\omega \backslash t$	3	6	7	8	9	10	11	12	13	14	15	16	17	18	19	20	21	22	23
0.08	0.41	1.44			3.04			4.48			5.57			6.21	6.33	6.38	6.42	6.42	6.39
0.10	0.52	1.81			3.73			5.36			6.38			6.66			6.23		
0.12	0.61	2.11			4.29			5.96	6.37	6.61	6.73	6.72	6.61		6.13			4.66	
0.14	0.71	2.42			4.82	5.44	6.47	6.41	6.73	6.83			6.13			4.31			
0.16					5.25	5.86	6.32	6.66	6.83	6.72									
0.18				4.84	5.61	6.15	6.52	6.71	6.67										
0.20			4.20	5.14	5.88	6.34	6.55	6.55											

Table 5: Elevations at  $(\frac{1}{2}\pi, 0)$ . Windfield  $\begin{cases} U = 0 \\ V = -\sin \omega t \end{cases}$  for various values of  $\omega$ ,  
Exponential bottom profile.  $\lambda = 0.12$ ,  $\Omega = 0.6$



## 6. The relaxation effect

In order to estimate the after-effect of a disturbance, say at  $t=0$ , we considered the model of a step-function windfield of the following type

$$U = 0, \quad V \begin{cases} = -1 & \text{for } t < 0 \\ = 0 & \text{" } t > 0, \end{cases}$$

upon the rectangular model with the exponential depth (1.6). This means that at  $t=0$  the elevation assumes its stationary value of

$$\zeta(x, y) = \int_y^b \frac{dy}{gh}.$$

From the numerous data obtained by the electronic computer we give here only the values of  $\zeta(\frac{1}{2}\pi, 0, t)$  at various times. They are given in table 6 and plotted in figure 8 (p. 24).

t	0	3	6	9	12	15	18	21	24
$\zeta(\frac{1}{2}\pi, 0, t)$	6.28	3.20	0.08	-0.96	-1.30	0.06	0.01	0.13	0.15

Table 6: Relaxation effect after the windfield  $U=0$ ,  $V = \begin{cases} -1 & (t < 0) \\ 0 & (t > 0) \end{cases}$

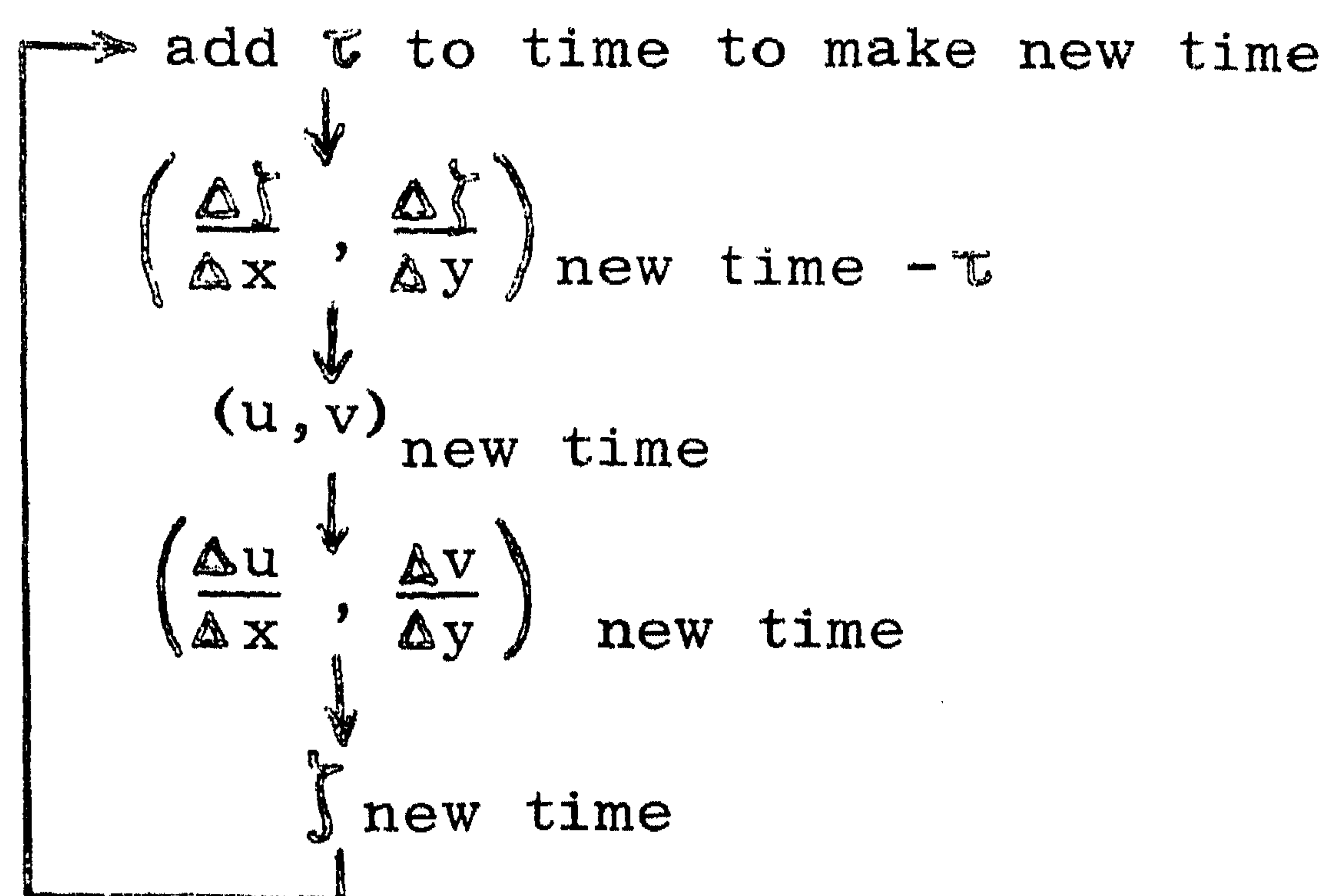
Exponential bottom profile,  $\lambda=0.12$ ,  $\Omega=0.6$ .

Apparently at  $t=0$  a wave is formed which travels from the coast  $y=0$  to the ocean  $y=2\pi$ , is reflected there at  $t=2\pi$  and returns at  $t=4\pi$  at the coast  $y=0$  where it interferes with the elevation present there. After  $t=15$  (in this model abt. 21 hours) the disturbance may be considered as practically having disappeared.

## 7. The ALGOL program

The ALGOL program given below is the equivalent of the program we actually used, which was coded in direct machine instructions for the X1 computer of the Mathematical Centre.

The program essentially runs through the same cycle once every time step  $\tau$ . This cycle can be represented as follows:



First we give a list of the symbols used in the program, then the program itself is given in the form of a procedure.

Symbols used in the procedure rectangularsea:

m,n: as used in (2.3)

i: counts the number of elementary time steps between times t and t+1

t: counts the number of time units

j,k: variables used to denote array indices

mmone, mmtwo, nmone, jmone, kmone: m-1, m-2, n-1, j-1, k-1 respectively

led:  $1/\tau$

dix:  $1/2\zeta = 1/\Delta x$

diy:  $1/2\eta = 1/\Delta y$

uh,vh: auxiliary variables

l:  $\lambda$

del:  $\tau$

halfdel:  $\frac{1}{2}\tau$

om :  $\Omega$

tw : auxiliary variable which is given the instantaneous value of  $F(t)$  \*)

timewind: the time-dependent component  $F(t)$  of the windfield  $(U,V)$  \*)

horwind: the (x,y) dependent part of the component of the wind in the x-direction  $U$  \*)

vertwind: " " " " " " " " the wind in the y-direction  $V$  \*)

u,v: components of the stream in the x and y directions respectively

z: elevation }

ux,vy,zx,zy:  $\frac{\Delta u}{\Delta x}, \frac{\Delta v}{\Delta y}, \frac{\Delta \zeta}{\Delta x}, \frac{\Delta \zeta}{\Delta y}$  respectively

half depth:  $\frac{1}{2}gh(x,y)$  for those values of (x,y) for which u and v are computed. .

-----  
\*) The windfield is represented by the vector  $(U(x,y)F(t), V(x,y)F(t))$ .



procedure rectangularsea; comment We omit input and output of data. It is assumed that the elements of the

procedure rectangularsea; comment We omit input and output of data. It is assumed that the elements of the arrays  $u, v$ , and  $z$  are given their initial values (usually zero), and that the elements of the arrays  $horwind$ ,  $vertwind$  and  $halfdepth$  are given the desired values.

Furthermore, that  $m, n, del, l$  and  $om$  are assigned the correct values;

integer  $m, n, i, t, j, k, led, nmone, nmtwo, nmone, jmcne, kmone;$

real  $dix, diy, uh, vh, l, om, del, halfdel, tw;$

array  $u, v, horwind, vertwind, halfdepth[0:m, 0:n];$

$z, ux[0:m-1, 0:n],$

$vy[0:m, 0:n-1],$

$zx[0:m-2, 0:n],$

$zy[0:m-1, 0:n-1];$

real procedure timewind( $i, t$ ); value  $i, t$ ; integer  $i, t$ ;

begin comment We omit the contents of the procedure body, which should assign to the procedure identifier timewind the instantaneous value of some function of  $t$ ;

end;

$dix := m / 3.141592653589793;$

$diy := .5 \times (2 \times r + 1) / 6.283185307179586;$

$i := t := 0;$

$led := 1.0 / del;$

$halfdel := .5 \times del;$

$nmone := m - 1; nmtwo := m - 2; nmone := n - 1;$

$i := i + 1; \text{if } i = led \text{ then begin } t := t + 1; i := 0 \text{ end;}$

$tw := timewind(i, t);$

for  $k := 0$  step 1 until  $n$  do

for  $j := 0$  step 1 until  $nmtwo$  do

$zx[j, k] := dix \times (z[j+1, k] - z[j, k]);$

for  $j := 0$  step 1 until  $nmone$  do

for  $k := 0$  step 1 until  $nmone$  do

$zy[j, k] := diy \times (z[j, k+1] - z[j, k]);$

```

for j:=1 step 1 until mmone do
  begin
    uh:=u[j,0]; jmone:=j-1;
    u[j,0]:=uh+delx(-lxuh-(3.0xzx[jmone,0]-zx[jmone,1])xhalfdepth[j,0]+horwind[j,0]xtw)
  end;
for k:=1 step 1 until n do
  begin
    vh:=v[m,0]; kmone:=k-1;
    v[0,k]:=vh+delx(-lxvh-(3.0xzy[0,kmone]-zy[1,kmone])xhalfdepth[0,k]+vertwind[0,k]xtw);
    for j:=1 step 1 until mmone do
      begin
        uh:=u[j,k]; vh:=v[j,k]; jmone:=j-1;
        u[j,k]:=uh+delx(-lxuh+cmxvh-(zx[jmone,k]+zx[jmone,kmone])x
          halfdepth[j,k]+horwind[j,k]xtw);
        v[j,k]:=vh+delx(-lxvh-cmxvh-(zy[j,kmone]+zy[jmone,kmone])x
          halfdepth[j,k]+vertwind[j,k]xtw)
      end;
    vh:=v[m,k]; v[m,k]:=vh+delx(-lxvh-(3.0xzy[mmone,kmone]-zy[mmtwo,kmone])xhalfdepth[m,k]+
      vertwind[m,k]xtw)
  end;
end;
for k:=0 step 1 until n do
  for j:=0 step 1 until mmone do
    ux[j,k]:=dixx(u[j+1,k]-u[j,k]);
  for j:=0 step 1 until m do
    for k:=0 step 1 until mmone do
      vy[j,k]:=diyx(v[j,k+1]-v[j,k]);
    for k:=0 step 1 until mmone do
      for j:=0 step 1 until mmone do
        z[j,k]:=z[j,k]-halfdelx(ux[j,k]+ux[j,k+1]-vy[j,k]+vy[j+1,k]);
      goto CYCLE;
    end;

```



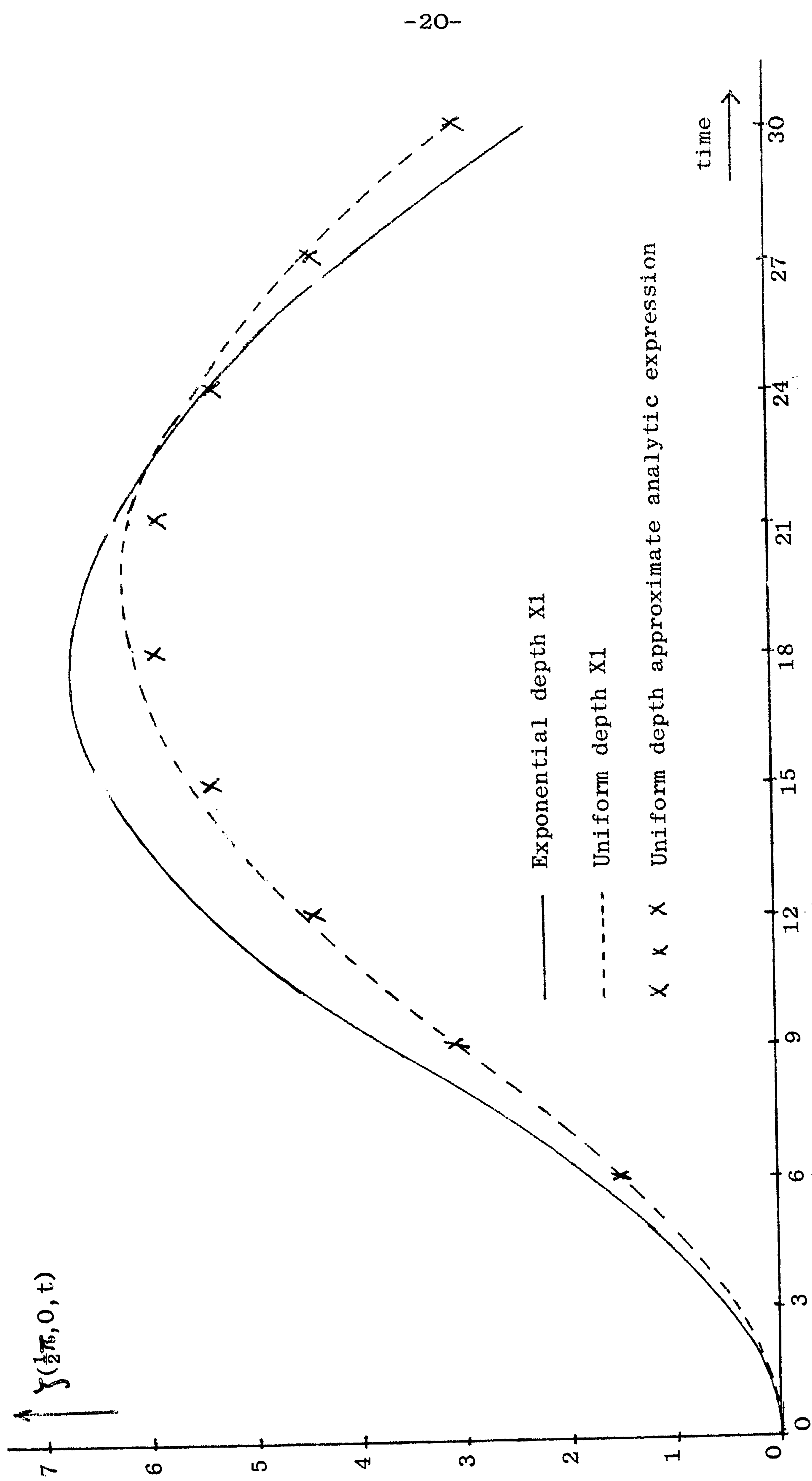


fig.2. Elevation at  $(\frac{1}{2}\pi, 0)$ . Windfield  $U=0$ ,  $V=-\sin 0.1t$

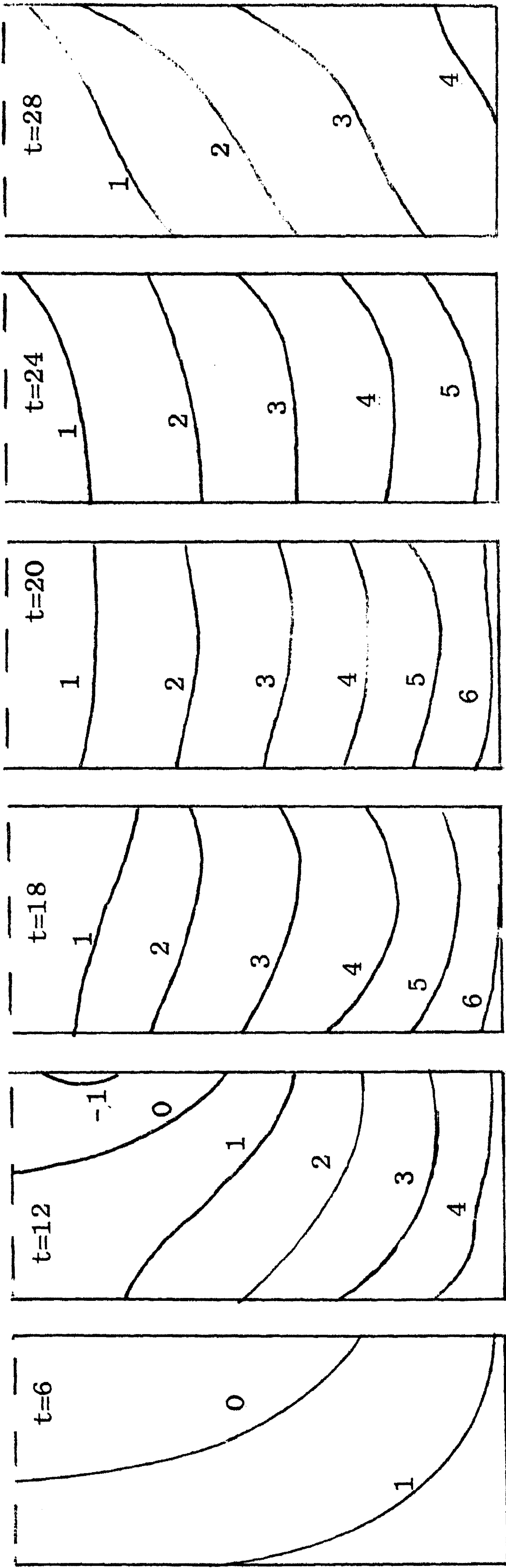


fig.3. Uniform depth. Isohypsyes due to the windfield  $U=0$ ,  $V=-\sin 0.1t$

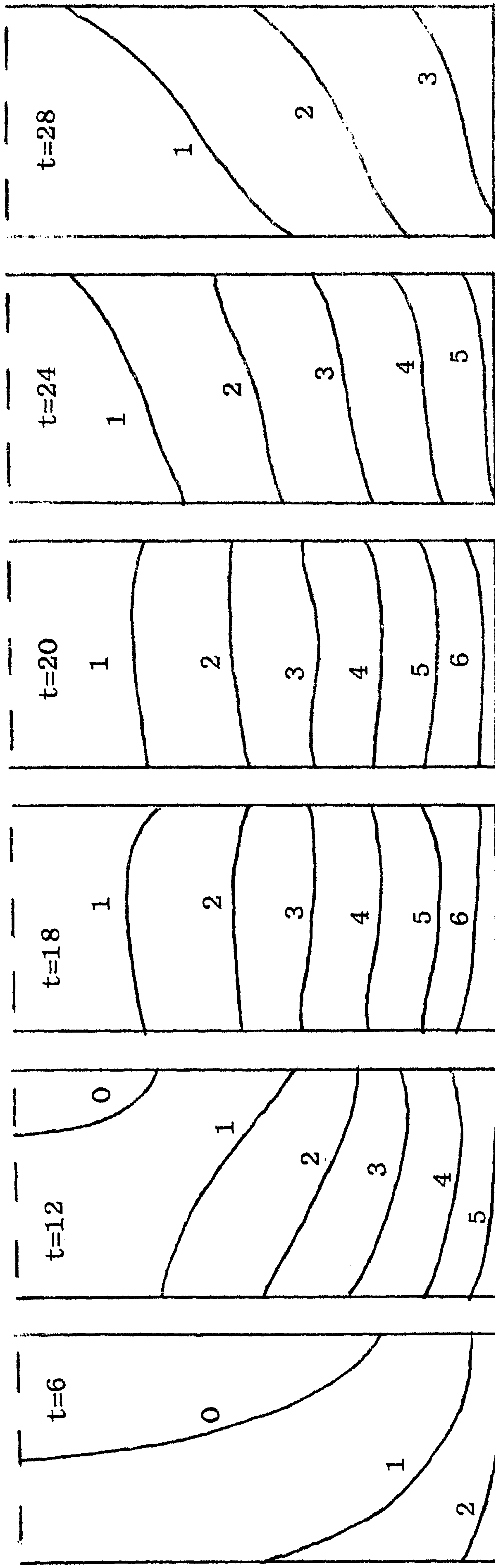


fig.4. Exponential depth. Isohypsyes due to windfield  $U=0$ ,  $V=-\sin 0.1t$



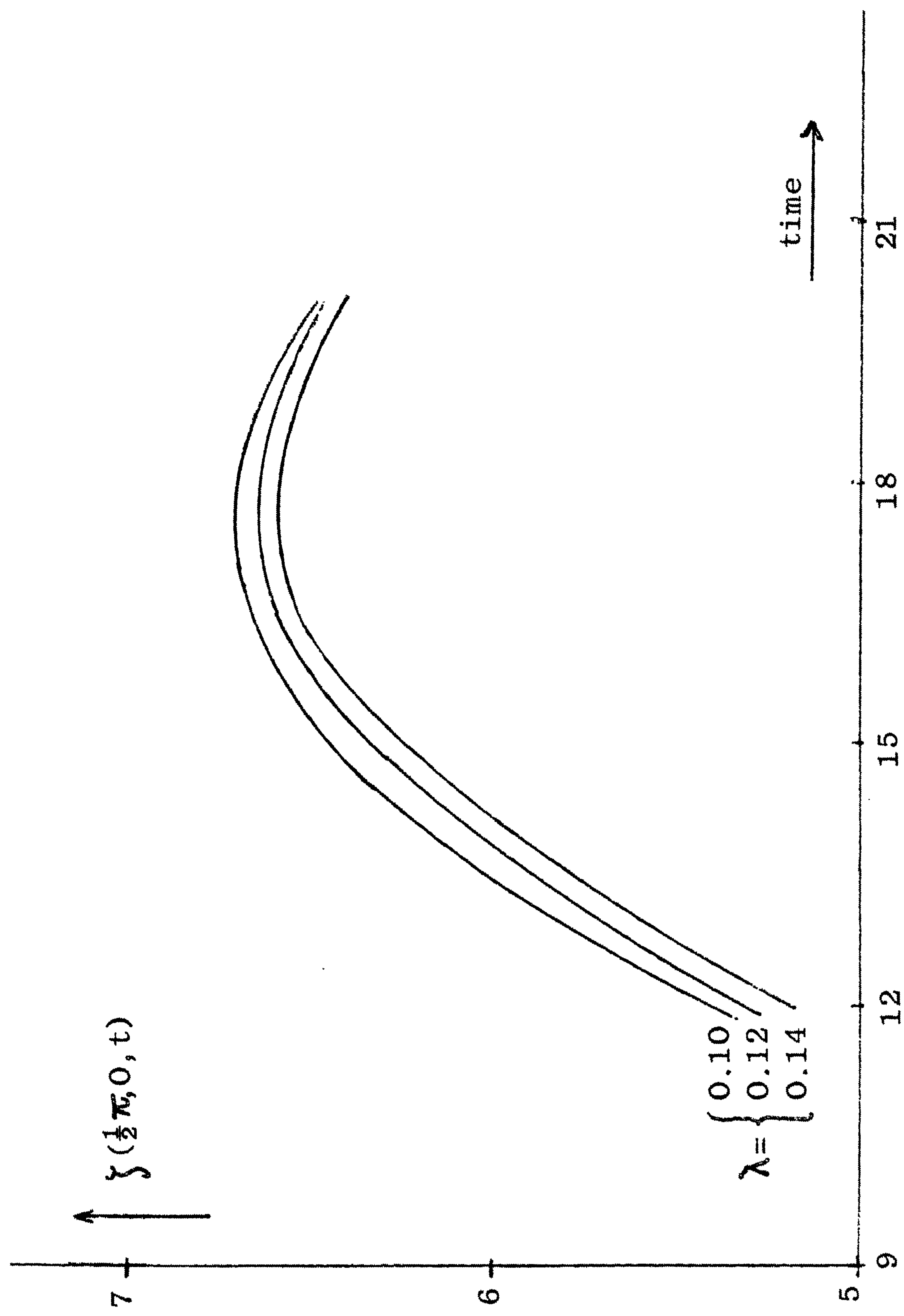


fig.5. Elevation at  $(\frac{1}{2}\pi, 0)$  Exponential depth Windfield  $U = 0$   $V = -\sin 0.1t$

$\Omega = 0.6$ , various values of  $\lambda$ .

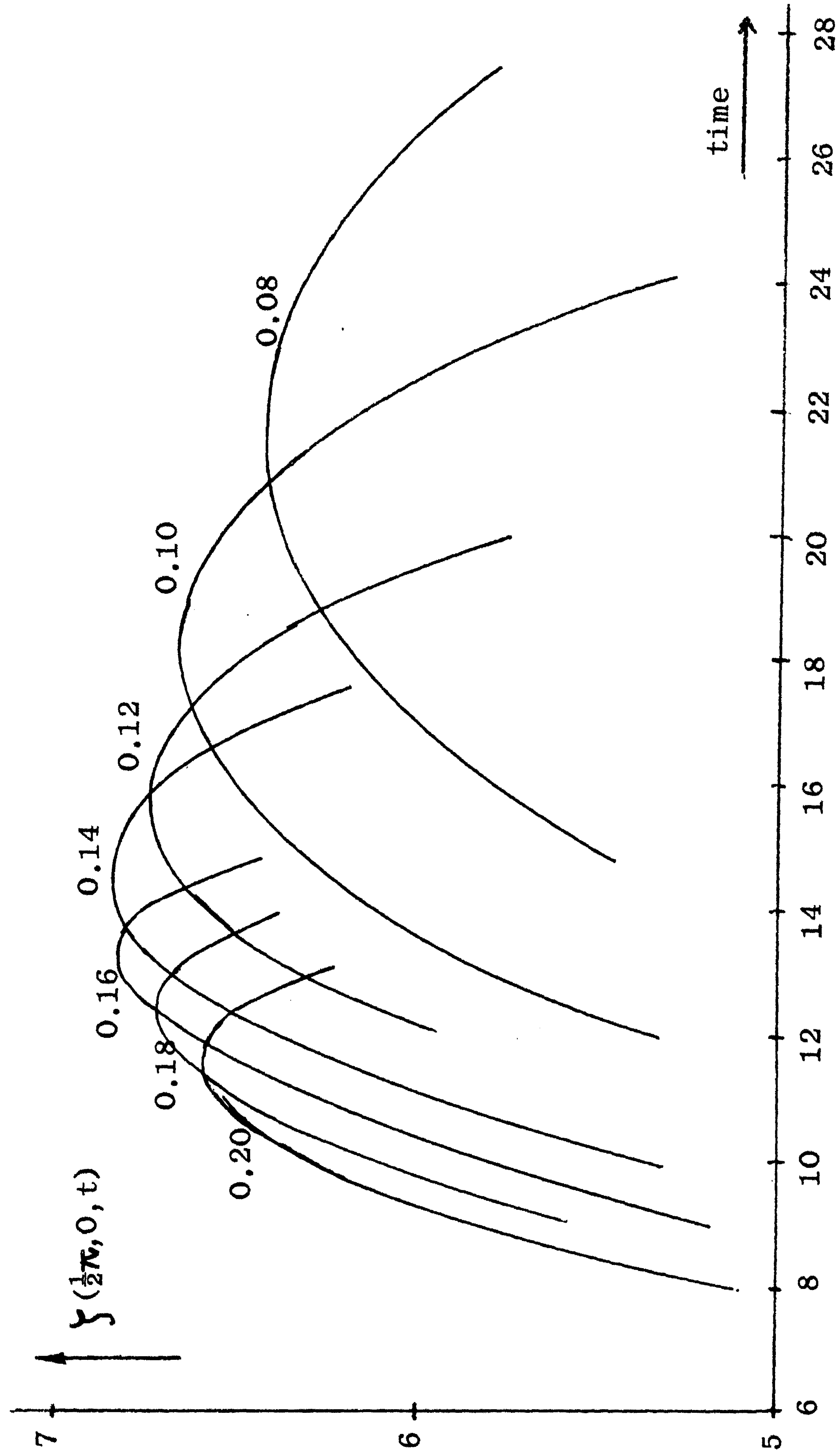


fig.6. Influence of  $\omega$  on the elevation at  $(\frac{1}{2}\pi, 0)$

Exponential depth, windfield  $U = 0$ ,  $V = -\sin \omega t$  for various values of  $\omega$ .

$\lambda = 0.12$ ,  $\Omega = 0.6$



fig.7. Influence of  $\omega$  on maximal elevation at  $(\frac{1}{2}\pi, 0)$

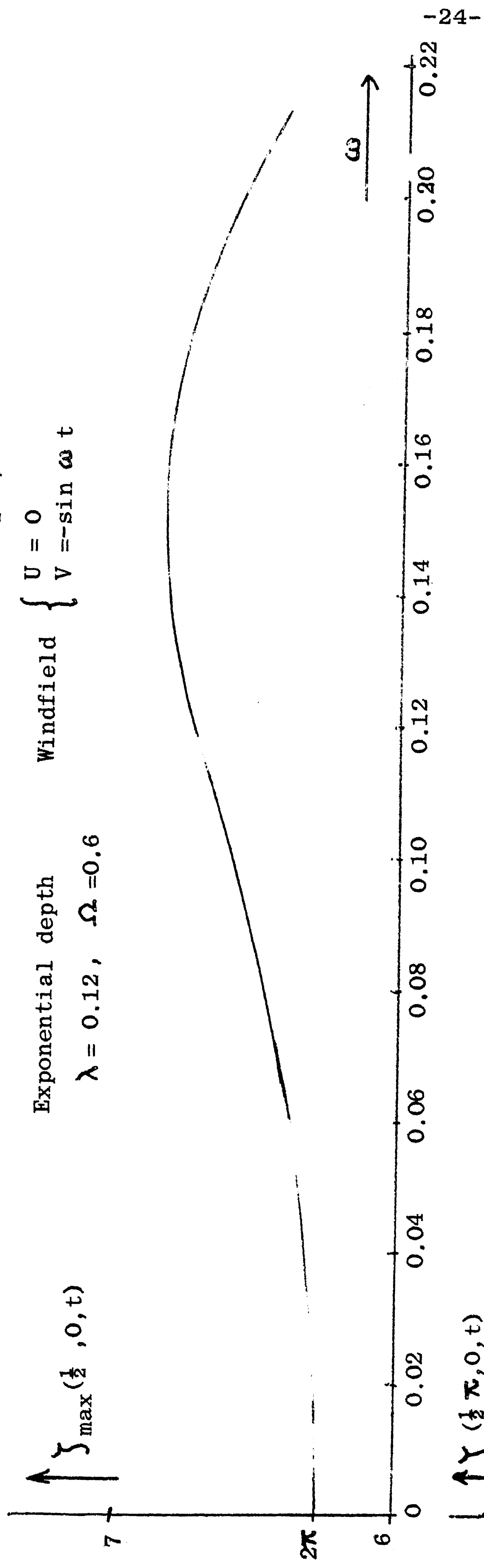


fig.8. The relaxation effect

Exponential depth  $\lambda = 0.12, \Omega = 0.6$

Windfield  $\begin{cases} U = 0 \\ V = \begin{cases} -1 & (t < 0) \\ 0 & (t \geq 0) \end{cases} \end{cases}$

